

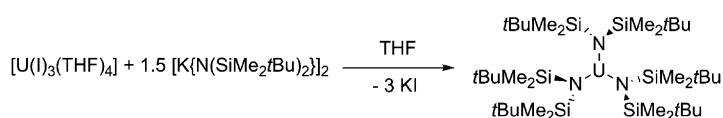
Ligand Effects | *Very Important Paper*VIP $[U^{III}\{N(SiMe_2tBu)_2\}_3]$: A Structurally Authenticated Trigonal Planar Actinide ComplexConrad A. P. Goodwin,^[a] Floriana Tuna,^[a] Eric J. L. McInnes,^[a] Stephen T. Liddle,^[b] Jonathan McMaster,^[b] Inigo J. Vitorica-Yrezabal,^[a] and David P. Mills^{*[a]}

Abstract: We report the synthesis and characterization of the uranium(III) triamide complex $[U^{III}(N^{**})_3]$ (**1**, $N^{**} = N(SiMe_2tBu)_2^-$). Surprisingly, complex **1** exhibits a trigonal planar geometry in the solid state, which is unprecedented for three-coordinate actinide complexes that have exclusively adopted trigonal pyramidal geometries to date. The characterization data for $[U^{III}(N^{**})_3]$ were compared with the prototypical trigonal pyramidal uranium(III) triamide complex $[U^{III}(N^*)_3]$ ($N^* = N(SiMe_3)_2^-$), and taken together with theoretical calculations it was concluded that pyramidalization results in net stabilization for $[U^{III}(N^*)_3]$, but this can be overcome with very sterically demanding ligands, such as N^{**} . The planarity of **1** leads to favorable magnetic dynamics, which may be considered in the future design of U^{III} single-molecule magnets.

Investigations into low-coordinate metal complexes (defined herein as coordination number, $CN < 4$) are legion, because they can exhibit interesting properties,^[1] including small-molecule activation chemistry^[2] and single-molecule magnet (SMM) behavior.^[3] Low CN complexes usually contain sterically demanding ligands to prevent oligomerization,^[1] in which bulky monodentate amides are frequently utilized.^[4] The bulky silylamide $\{N(SiMe_3)_2\}^-$ (N^*) has provided landmark low CN complexes; for example, three-coordinate $[M^{III}(N^*)_3]$ complexes of Group 13 ($M = Al, Ga, In, Tl$)^[5] and first row d-block ($M = Ti-Co$)^[6] metals are trigonal planar (D_{3h}) in the solid state, but Group 3,^[6a,7] lanthanide (Ln),^[7] and actinide (An)^[8] $[M^{III}(N^*)_3]$ complexes exhibit trigonal pyramidal (C_{3v}) solid-state geometries, although they have zero dipole moment in solution, inferring

that they may become planar in this phase.^[9] Pyramidal geometries persist for $[Ln^{III}(N^*)_3]$ ($Ln = Ce, Pr$) in the gas phase,^[10] but $[Sc^{III}(N^*)_3]$ vapors are D_{3h} , with crystalline/gas-phase discrepancies for this complex attributed to crystal-packing effects.^[11] It is noteworthy that complexes, such as $[Ln^{III}(N^*)(\mu-N^*)_2Na]$ ($Ln = Eu, Yb$) and $[Sm^{III}(N^*)(\mu-N^*)_2M]$ ($M = Na, K$), have trigonal planar Ln coordination spheres,^[12] but this geometry has not been previously observed in An complexes.

f-Block metal centers favor high CNs, because Ln and An cations have relatively large ionic radii and bonding regimes that are dominated by electrostatic contributions.^[13] Low CN U^{III} chemistry is burgeoning, driven by interesting small molecule activation reactions^[14] and intrinsic SMM behavior.^[15] Structurally characterized three-coordinate An complexes to date adopt exclusively trigonal pyramidal geometries rather than trigonal planar or T shaped (C_{2v}),^[16] although matrix isolation experiments^[17] and calculations^[18] have shown that monomeric UO_3 is T shaped. Both covalent^[19] and electrostatic^[10] arguments account for the trigonal pyramidal geometry of $[U^{III}(N^*)_3]$,^[8,20] hence, the most influential factor of these two for causing pyramidalization has never been established. Herein, we report the structurally characterized An complex, $[U^{III}(N^{**})_3]$ (**1**, $N^{**} = N(SiMe_2tBu)_2^-$), which adopts an unprecedented trigonal planar geometry for an actinide triamide complex. Complex **1** is closely related to $[U^{III}(N^*)_3]$, allowing the contributions to pyramidalization to be assessed, together with the impact of geometry

Scheme 1. Synthesis of **1**.

[a] C. A. P. Goodwin, Dr. F. Tuna, Prof. E. J. L. McInnes, Dr. I. J. Vitorica-Yrezabal, Dr. D. P. Mills
School of Chemistry, The University of Manchester
Oxford Road, Manchester, M13 9PL (UK)
E-mail: david.mills@manchester.ac.uk

[b] Prof. S. T. Liddle, Dr. J. McMaster
School of Chemistry, The University of Nottingham
University Park, Nottingham, NG7 2RD (UK)

Supporting information for this article is available on the WWW under <http://dx.doi.org/10.1002/chem.201404864>.

© 2014 The Authors. Published by Wiley-VCH Verlag GmbH & Co. KGaA. This is an open access article under the terms of the Creative Commons Attribution License, which permits use, distribution and reproduction in any medium, provided the original work is properly cited.

on magnetic (including dynamic) and electronic properties of U^{III} complexes, for the future rational design of useful An materials.

Complex **1** was prepared by a modification of the revised synthesis of $[U^{III}(N^*)_3]$.^[8c] Compound $[U^{III}(l)_3(THF)_4]$ ^[8c] was reacted with 1.5 equivalents of $[K\{N(SiMe_2tBu)_2\}]_2$ in THF, followed by work-up and recrystallization from hexane to give **1** as dark purple needles in 62% yield (Scheme 1).^[21] Absorbances in the FTIR spectrum of **1** at $\tilde{\nu} = 950, 825,$ and 761 cm^{-1} are attributed to the $UNSi_2$ stretching modes of the silylamide ligand. The asymmetric stretch (950 cm^{-1}) is 40 cm^{-1} lower than that observed for $[U^{III}(N^*)_3]$ (990 cm^{-1}),^[8a] which is of a similar magni-

tude to the differences between previously reported planar and pyramidal $[M(N^{\nu})_3]$ $MNSi_2$ asymmetric stretches (ca. 50 cm^{-1}).^[5b,6a]

The ^1H NMR spectrum of **1** exhibits two resonances at $\delta = 3.8$ ($\nu^{1/2} = 206\text{ Hz}$) and -47.0 ppm ($\nu^{1/2} = 4597\text{ Hz}$) in a 54:36 ratio that are assigned to the *t*BuSi and Me_2Si protons, respectively. The Me_2Si resonance of **1** is much broader than the analogous resonance for $[\text{U}^{\text{III}}(\text{N}^{\nu})_3]$ ($\delta = -11.4$, $\nu^{1/2} = 15\text{ Hz}$),^[8] but variable-temperature (VT) studies gave a sharper resonance at 353 K ($\delta = -32.9\text{ ppm}$, $\nu^{1/2} = 266\text{ Hz}$).^[21] A wide-scan ^{13}C NMR spectrum of **1** exhibited two resonances for the Me_2Si ($\delta = -2.1$ and 1.5 ppm) and *t*BuSi quaternary carbons ($\delta = 18.2$ and 32.0 ppm), but only one for the *t*BuSi primary carbons ($\delta = 26.4\text{ ppm}$). In contrast, in the ^{13}C NMR spectrum of $[\text{U}^{\text{III}}\{\text{N}(\text{SiPhMe}_2)_2\}_3]$, the Me_2Si group resonates at $\delta = -57.1\text{ ppm}$.^[22] A resonance was observed in the ^{29}Si NMR spectrum of **1** at $\delta = -296.0\text{ ppm}$ ($\nu^{1/2} = 73\text{ Hz}$), which has not been reported for similar systems,^[8,22] but is typical for a U^{III} complex.^[23]

The electronic absorption spectrum of **1**^[21] exhibited $5f^2 \rightarrow 5f^2 6d^1$ transitions at 20000 ($\epsilon = 776\text{ M}^{-1}\text{ cm}^{-1}$) and 22500 cm^{-1} ($\epsilon = 770\text{ M}^{-1}\text{ cm}^{-1}$) that are typical of U^{III} ^[24] and comparable to a broad absorption observed for $[\text{U}^{\text{III}}\{\text{N}(\text{SiPhMe}_2)_2\}_3]$ at 21500 cm^{-1} ($\epsilon = 430\text{ M}^{-1}\text{ cm}^{-1}$).^[22] In the $7000\text{--}13000\text{ cm}^{-1}$ region, weak Laporte forbidden $5f \rightarrow 5f$ transitions were observed ($\epsilon = 15\text{--}64\text{ M}^{-1}\text{ cm}^{-1}$).^[25] Similar weak absorptions were observed for most U^{III} complexes, such as $[\text{U}(\text{I})_3(\text{THF})_4]$ ^[8c,26] and $[\text{U}^{\text{III}}\{\text{N}(\text{SiPhMe}_2)_2\}_3]$,^[22] and strong absorptions in this region are very rare.^[27]

The crystal structure of **1** was determined and is depicted in Figure 1, with selected metrical parameters.^[28] Complex **1** crystallizes in the $C2/c$ space group, with a twofold axis bisecting the $\text{U}(1)\text{--N}(1)$ bond. This contrasts to $[\text{Fe}(\text{N}^{\nu})_3]$,^[9] $[\text{Eu}^{\text{III}}(\text{N}^{\nu})_3]$,^[29] $[\text{U}^{\text{III}}(\text{N}^{\nu})_3]$,^[8d] and $[\text{Pu}^{\text{III}}(\text{N}^{\nu})_3]$,^[8e] which all crystallize exclusively in the $P3_1c$ space group, and $[\text{U}^{\text{III}}\{\text{N}(\text{SiPhMe}_2)_2\}_3]$, which crystallizes in $R3$.^[22] The U atom of **1** is almost ideally trigonal planar, with U–N bonds that are statistically identical within experimental uncertainty [U–N range $2.403(3)\text{--}2.415(6)\text{ \AA}$]. These distances are longer than those observed in $[\text{U}^{\text{III}}(\text{N}^{\nu})_3]$ [$2.320(4)\text{ \AA}$]^[8d] and $[\text{U}^{\text{III}}\{\text{N}(\text{SiPhMe}_2)_2\}_3]$ [$2.34(2)\text{ \AA}$],^[22] which can be attributed to the greater interligand repulsion in **1** arising from the sterically demanding *t*Bu groups. The U centroid/ $\text{N}(1)\text{--N}(2)\text{--N}(2\text{A})$ mean plane distance in **1** is $0.008(2)\text{ \AA}$, and the N–U–N bond angles (range $119.1(2)\text{--}120.47(9)^\circ$) sum to 360° ; in contrast, $[\text{U}^{\text{III}}(\text{N}^{\nu})_3]$ and $[\text{U}^{\text{III}}\{\text{N}(\text{SiPhMe}_2)_2\}_3]$ exhibit U centroids $0.456(1)$ and 0.874 \AA from the N_3 planes, and the N–U–N angles average $116.24(7)$ (Σ angles $348.72(7)^\circ$) and 106.88° (Σ angles 320.64°), respectively.^[8d,22] The UNSi_2 fragments of **1** are essentially planar and all bisect the UN_3 plane (range $53.23\text{--}61.35^\circ$) to form a molecular propeller.

The pyramidal geometries of $[\text{U}^{\text{III}}(\text{N}^{\nu})_3]$ and $[\text{U}^{\text{III}}\{\text{N}(\text{SiPhMe}_2)_2\}_3]$ are predicted by the polarized-ion model, whereby net stabilization was achieved by dipole formation.^[8d,22] $[\text{U}^{\text{III}}(\text{N}^{\nu})_3]$ exhibits unequal U–N–Si angles ($108.50(7)$ and $125.25(7)^\circ$), because one Si–C bond for each N^{ν} ligand is relatively close to the U center [U...C $_{\gamma}$ 3.05 \AA ; U...Si 3.29 \AA].^[8d] These can be attributed to stabilizing agostic M...Si–C $_{\gamma}$ interactions, as have been discussed for $[\text{U}^{\text{III}}\{\text{CH}(\text{SiMe}_3)_2\}_3]$ ^[30] and $[\text{Sm}^{\text{III}}(\text{N}^{\nu})_3]$.^[31] The shortest U...C $_{\gamma}$ and

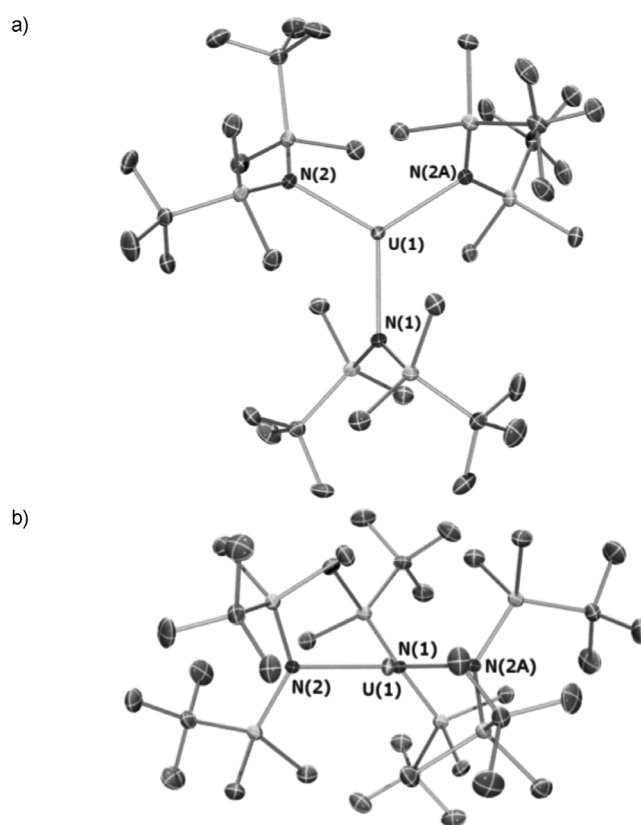


Figure 1. Molecular structures of **1** a) top view and b) along twofold axis, with selected atom labelling. Displacement ellipsoids are set at the 40% probability level, and hydrogen atoms are removed for clarity. Selected bond lengths [\AA] and angles [$^\circ$]: $\text{U}(1)\text{--N}(1)$ $2.403(3)$, $\text{U}(1)\text{--N}(2)$ $2.415(6)$; $\text{N}(1)\text{--U}(1)\text{--N}(1')$ $119.05(19)$, $\text{N}(1)\text{--U}(1)\text{--N}(2)$ $120.47(9)$.

U...Si distances in **1** are $3.119\text{--}3.301\text{ \AA}$ and $3.433\text{--}3.510\text{ \AA}$, respectively, and they are not correctly orientated to interact with the U center. Although there is no evidence for agostic U...Si–C $_{\gamma}$ interactions in **1**, stabilizing U...C–H contacts cannot be discounted.

Unrestricted DFT calculations were carried out on full models of **1** and $[\text{U}^{\text{III}}(\text{N}^{\nu})_3]$.^[21] The geometry-optimized structures reproduce the experimental structures with good agreement, despite the slight deviation from planarity for the model of **1** (discrepancies attributed to this being a gas-phase calculation, which does not account for crystal-packing forces), providing qualitative models (bond lengths within 0.05 \AA , angles within 1° , U centroid/ N_3 mean plane distance: **1** 0.132 \AA , $[\text{U}^{\text{III}}(\text{N}^{\nu})_3]$ 0.393 \AA). In both models, the HOMO, HOMO–1 and HOMO–2 represent the three unpaired U^{III} 5f electrons (**1**: 93.93, 94.71, 90.09; $[\text{U}^{\text{III}}(\text{N}^{\nu})_3]$ 86.81, 86.32, 84.17% U 5f, respectively). Both models exhibit essentially insignificant degrees of U 6d/5f orbital contributions to the U–N bonds, with the HOMO–3, HOMO–4, and HOMO–5, representing the π components (**1**: 5.27/0, 1.57/0, 0/1.31; $[\text{U}^{\text{III}}(\text{N}^{\nu})_3]$ 4.29/0, 0/2.06, 1.63/1.39% U 5f/6d, respectively) and the HOMO–6, HOMO–7, and HOMO–8 the σ components (**1**: 0/2.29, 0/2.12, 1.20/0; $[\text{U}^{\text{III}}(\text{N}^{\nu})_3]$ 0/5.04, 0/5.26, 2.14/0% U 5f/6d, respectively). This concurs with gas-phase photoelectron spectroscopy (PES) studies of

$[\text{U}(\text{N}^*)_3]$, which have shown that π bonding between the ligand and U center is insignificant in this complex.^[32] The calculated uranium spin densities (MDC-m α spin, $1 = -3.26$; $[\text{U}^{\text{III}}(\text{N}^*)_3] = -3.26$) are identical, which also supports similar bonding patterns for **1** and $[\text{U}^{\text{III}}(\text{N}^*)_3]$.

Ab initio calculations on $[\text{An}^{\text{III}}(\text{CH}_3)_3]$ (An = U, Np, Pu)^[33] and $[\text{An}^{\text{III}}(\text{NH}_2)_3]$ (An = U, Np)^[34] have shown that the involvement of An 6d orbitals in the U–X (X = C, N) σ components may be associated with pyramidalization in the absence of steric contributions. Thus, given the similar bonding within **1** and $[\text{U}^{\text{III}}(\text{N}^*)_3]$ together with the small U 6d/5f contributions to the U–N σ and π components, we suggest that the experimentally determined trigonal planar geometry of **1** results from steric interactions involving the large N** ligands. These interactions could predominate over crystal packing forces, which are often only approximately 10 kJ mol⁻¹.^[35] We conclude that there are minor differences in bonding between **1** and $[\text{U}^{\text{III}}(\text{N}^*)_3]$, therefore, the planar geometry of **1** derives principally from steric effects involving the ligands.

The solution magnetic moment of **1** was calculated to be 2.59 μ_B in $[\text{D}_6]$ benzene at 298 K by using the Evans method.^[36] Magnetometry measurements on a powdered sample of **1** suspended in eicosane gave a magnetic susceptibility temperature product, χT , of 1.07 cm³ K mol⁻¹ (2.92 μ_B) at 298 K,^[21] which corresponds well with the solution measurement considering weighing errors and the difference in phase. These values are lower than for a free-ion 5f³ ⁴_{1/2} ground state (3.69 μ_B), because not all crystal field levels are thermally occupied,^[37] but are typical for U^{III} complexes described in the literature (range 2.13–4.63 μ_B).^[8,15,22,25,26,30,38] The χT value of **1** decreases to 0.41 cm³ K mol⁻¹ at 2 K; ac measurements give a low-temperature plateau in the in-phase χ'/T at 0.48 cm³ K mol⁻¹^[21] consistent with thermal depopulation into a Kramers doublet ground state.^[3,13] Low-temperature EPR spectra of **1** are consistent with U^{III},^[27] and simulation gives $g_{\text{eff}} = 3.55, 2.97, \text{ and } 0.553$ for the ground Kramers doublet (the latter is observed at high field at X-band, but is beyond the magnetic field range at Q band; Figure 2a).

Compound $[\text{U}^{\text{III}}(\text{N}^*)_3]$ is an SMM,^[15] hence, we have performed low-temperature ac measurements on **1** to probe differences in the dynamic magnetic behavior as a result of the higher symmetry. Compound **1** is also an SMM, with clear frequency-dependent behavior (Figure 2c and d).^[21] Under the optimal dc field of 600 G, the magnetization relaxes much slower than in $[\text{U}^{\text{III}}(\text{N}^*)_3]$, and maxima in the out-of-phase susceptibility $\chi''(T)$ are seen to significantly higher temperatures for **1** than for $[\text{U}^{\text{III}}(\text{N}^*)_3]$ at equivalent frequencies (e.g., 3.5 vs. 2.1 K, respectively, for 1.4 kHz). An Arrhenius treatment^[21] of the higher-temperature ac data gives an energy barrier of $U_{\text{eff}} = 21.4 \pm 0.2$ K for **1**. Although this is lower than that reported for $[\text{U}^{\text{III}}(\text{N}^*)_3]$ (31 K), the latter value was derived from an extremely limited temperature range^[15] and should be treated with some caution. The relaxation time (τ) at 2 K is 2.6 ms for **1**; from the previously reported data^[15] we find 0.3 ms for $[\text{U}^{\text{III}}(\text{N}^*)_3]$ at 2 K, an order of magnitude quicker. The pre-factor τ_0 for **1** is greater by four orders of magnitude (3.1×10^{-7} cf. 10^{-11} s for $[\text{U}^{\text{III}}(\text{N}^*)_3]$).^[15] Moreover, the frequency dependence of

χ' and χ'' at 1.8 K for **1**^[21] reveal a single relaxation process with a narrow distribution in relaxation times ($\alpha = 0.001$ –0.03 from Cole–Cole analysis), an order of magnitude lower than in $[\text{U}^{\text{III}}(\text{N}^*)_3]$ ($\alpha = 0.09$ –0.34).^[15] In fact, the difference in dynamics is sufficient that magnetization hysteresis is observed for **1** at 1.8 K on a conventional superconducting quantum interference device (SQUID) magnetometer (Figure 2b), while it is not for $[\text{U}^{\text{III}}(\text{N}^*)_3]$.

In the trigonal planar geometry of **1**, with no axial ligands, we expect a low J_z state of U^{III} to be stabilized by the crystal field. This is supported by the EPR analysis: if we assume a ⁴_{1/2} ground term,^[39] with $g_j = 8/11$, the $J_z = \pm 1/2$ doublet is calculated to have $g_{xy} = 3.65, g_z = 0.73$ (all other doublets have $g_{xy} = 0$), in good agreement with experiment. $|J_z| = 1/2$ is also the ground doublet of the (pyramidal) 4f³ complex $[\text{Nd}^{\text{III}}(\text{N}^*)_3]$ from optical studies.^[40] Hence, **1** and $[\text{U}^{\text{III}}(\text{N}^*)_3]$ are SMMs despite their easy-plane anisotropy: this highlights the complexity of interpreting f-block relaxation data,^[41] particularly when relatively low (tens of K) energy barriers are involved. At this stage, we can speculate that the “cleaner” and slower relaxation of **1** compared with $[\text{U}^{\text{III}}(\text{N}^*)_3]$ on flattening the geometry is because of quenched mixing. In D_{3h} $|J_z| = 1/2$ cannot mix with any other doublet within the ⁴_{1/2} term, whereas in C_{3v} it can mix with both $|J_z| = 5/2$ and $7/2$.

To conclude, we have prepared and fully characterized an unprecedented trigonal planar actinide triamide complex. Differences in the spectroscopic and magnetic data between **1** and $[\text{U}^{\text{III}}(\text{N}^*)_3]$ can be attributed to differences in symmetry that may be useful to consider in the future design of U^{III} SMMs with greater relaxation times. Computational analyses of **1** and $[\text{U}^{\text{III}}(\text{N}^*)_3]$ have shown only minor differences in their calculated bonding schemes, therefore, the energy gained by pyramidalization, which leads to favorable agostic M...Si–C_i interactions in $[\text{U}^{\text{III}}(\text{N}^*)_3]$,^[8d,32,33] can be overcome by sterically demanding ligands, such as N**.

Experimental Section

Synthesis of 1: THF (20 mL) was added to a precooled (–78 °C) mixture of $[\text{K}(\text{N}(\text{SiMe}_2\text{tBu})_2)_2]$ (1.007 g, 1.5 mmol) and $[\text{U}(\text{I}_3)(\text{THF})_4]$ (0.907 g, 1 mmol). The reaction mixture was allowed to warm to RT slowly with stirring over 48 h, with precipitation of a pale solid. Volatiles were removed in vacuo, and the dark purple solid was extracted with hexanes (3 × 10 mL). Recrystallization from hexanes (5 mL) at –30 °C gave **1** as dark purple needles (0.605 g, 62%). ¹H NMR (400.13 MHz, $[\text{D}_6]$ benzene, 25 °C, TMS): $\delta = -47.04$ (br s, $\nu^{1/2} = 4597$ Hz, 36 H; Si(CH₃)₂), 3.79 ppm (br s, $\nu^{1/2} = 206$ Hz, 54 H; SiC(CH₃)₃); ¹³C{¹H} NMR (100.61 MHz, $[\text{D}_6]$ benzene, 25 °C, TMS): $\delta = -2.13$ (Si(CH₃)₂), 1.45 (Si(CH₃)₂), 18.22 (SiC(CH₃)₃), 26.40 (SiC(CH₃)₃), 31.98 ppm (SiC(CH₃)₃); ²⁹Si{¹H} NMR (79.48 MHz, $[\text{D}_6]$ benzene, 25 °C, TMS): $\delta = -296.04$ ppm (br. s, $\nu^{1/2} = 73$ Hz); FTIR (Nujol): $\tilde{\nu} = 1259$ (s), 1247 (s), 1002 (s), 950 (m, asym. str., UNSi₂), 825 (s, sym. str., UNSi₂), 761 (s, sym. str., UNSi₂), 655 (m), 604 (s) cm⁻¹; $\mu_{\text{eff}} = 2.59 \mu_B$ (Evans method); elemental analysis calcd for C₃₆H₉₀Si₆N₃U (971.67 g mol⁻¹): C 44.5, H 9.34, N 4.33; found: C 38.29, H 9.10, N 4.22. Low carbon values were obtained upon repeating the analysis multiple times on different batches and is ascribed to **1** being a silicon-rich molecule, as was observed previously.^[42]

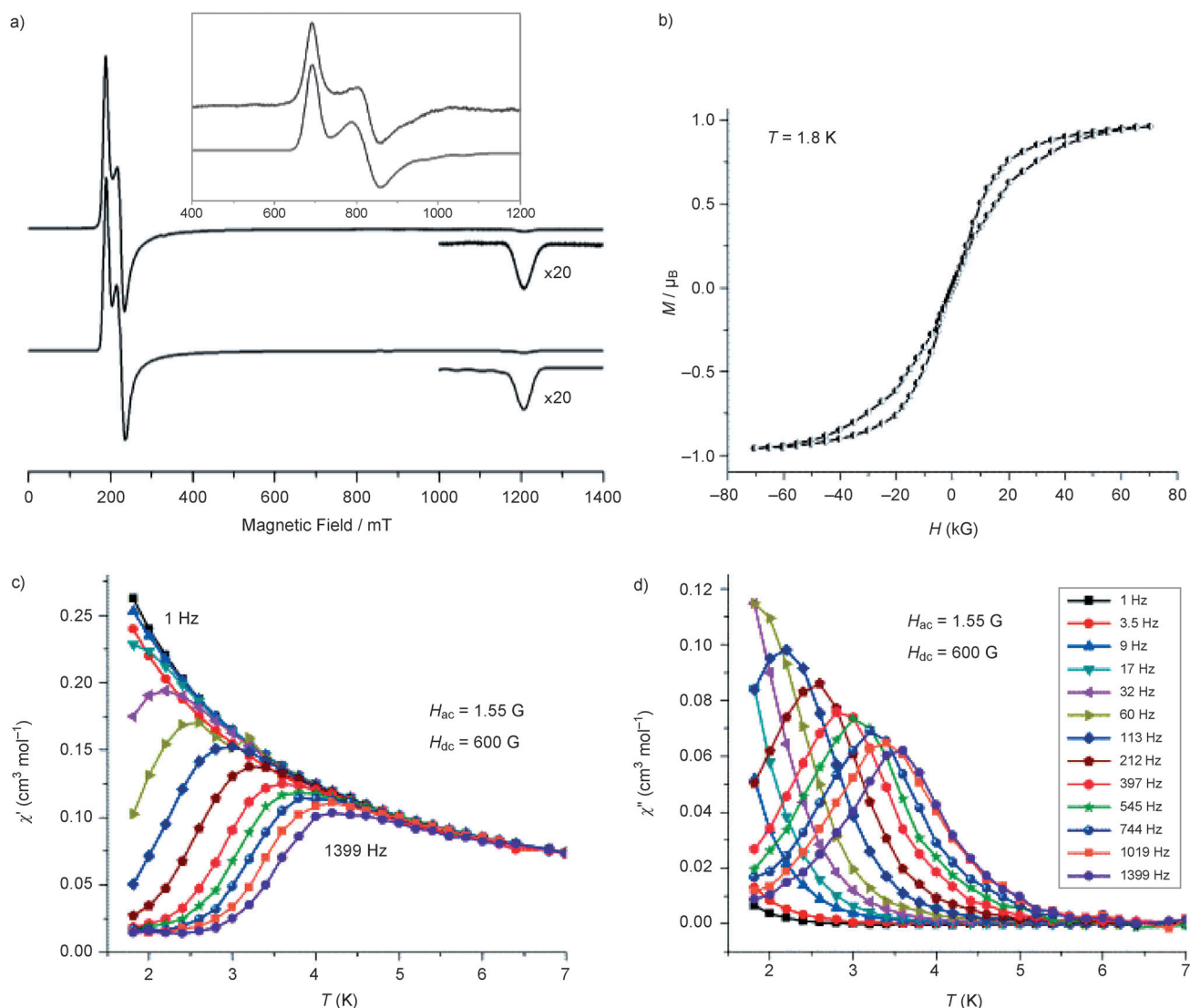


Figure 2. a) X- (9.5 GHz) and Q-band (34 GHz; inset) EPR spectra of **1** at 5 K. Lower spectra are simulations as $S_{\text{eff}} = 1/2$. Magnetic-susceptibility data for **1**: b) magnetic hysteresis at 1.8 K, sweep rate 13 G s^{-1} ; c) in-phase (χ'); and d) out-of-phase (χ'') components of the ac susceptibility measured in an applied dc field of 600 G and an oscillating field of 1.55 G.

Acknowledgements

We thank the EPSRC (grant numbers EP/L014416/1 and EP/K039547/1), including for the National EPR Facility, and The University of Manchester for funding this work.

Keywords: actinides · ligand design · ligand effects · single-molecule magnets · uranium

- [1] *Organometallics*, 3rd completely revised and extended edition (Ed.: C. Elschenbroich), Wiley-VCH, Weinheim, **2006**.
- [2] C. C. Lu, K. Meyer, *Eur. J. Inorg. Chem.* **2013**, 3731–3732, and references cited therein.
- [3] *Molecular Nanomagnets* (Eds.: D. Gatteschi, R. Sessoli, J. Villain), OUP, Oxford, **2006**.
- [4] a) *Metal and Metalloid Amides*, (Eds.: M. F. Lappert, P. P. Power, A. R. Sanger, R. C. Srivastava), Ellis Horwood-Wiley, Chichester, **1980**; b) R. Anwander, *Top. Curr. Chem.* **1996**, 179, 33–112; c) *Metal Amide Chemistry*

(Eds.: M. F. Lappert, A. Protchenko, P. Power, A. Seeber), Wiley, Chichester, **2008**.

- [5] a) J. Pump, E. G. Rochow, U. Wannagat, *Angew. Chem.* **1963**, 75, 374–375; b) H. Bürger, J. Cichon, U. Goetze, U. Wannagat, H. J. Wismar, *J. Organomet. Chem.* **1971**, 33, 1–12; c) P. Krommes, J. Lorberth, *J. Organomet. Chem.* **1977**, 131, 415–422.
- [6] a) E. C. Alyea, D. C. Bradley, R. G. Copperthwaite, *J. Chem. Soc. Dalton Trans.* **1972**, 1580–1584; b) J. J. Ellison, P. P. Power, S. C. Shoner, *J. Am. Chem. Soc.* **1989**, 111, 8044–8046.
- [7] D. C. Bradley, J. S. Ghotra, F. A. Hart, *J. Chem. Soc. Dalton Trans.* **1973**, 1021–1023.
- [8] a) R. A. Andersen, *Inorg. Chem.* **1979**, 18, 1507–1509; b) D. L. Clark, A. P. Sattelberger, S. G. Bott, R. N. Vrtis, *Inorg. Chem.* **1989**, 28, 1711–1733; c) L. R. Avens, S. G. Bott, D. L. Clark, A. P. Sattelberger, J. G. Watkin, B. D. Zwick, *Inorg. Chem.* **1994**, 33, 2248–2256; d) J. L. Stewart, R. A. Andersen, *Polyhedron* **1998**, 17, 953–958; e) A. J. Gaunt, A. E. Enriquez, S. D. Reilly, B. L. Scott, M. P. Neu, *Inorg. Chem.* **2008**, 47, 26–28.
- [9] J. S. Ghotra, M. B. Hursthouse, A. J. Welch, *J. Chem. Soc. Chem. Commun.* **1973**, 669–670.
- [10] T. Fjeldberg, R. A. Andersen, *J. Mol. Struct.* **1985**, 129, 93–105.
- [11] T. Fjeldberg, R. A. Andersen, *J. Mol. Struct.* **1985**, 128, 49–57.

- [12] a) T. D. Tilley, R. A. Andersen, A. Zalkin, *Inorg. Chem.* **1984**, *23*, 2271–2276; b) W. J. Evans, M. A. Johnston, R. D. Clark, R. Anwander, J. W. Ziller, *Polyhedron* **2001**, *20*, 2483–2490.
- [13] *The Chemistry of the Actinide and Transactinide Elements* (Eds.: L. R. Morss, N. M. Edelstein, J. Fuger), Springer, Dordrecht, **2006**.
- [14] a) H. S. La Pierre, K. Meyer, *Prog. Inorg. Chem.* **2014**, *58*, 303–416; b) B. M. Gardner, S. T. Liddle, *Eur. J. Inorg. Chem.* **2013**, 3753–3770; c) P. L. Arnold, *Chem. Commun.* **2011**, *47*, 9005–9010; d) I. Castro-Rodríguez, K. Meyer, *Chem. Commun.* **2006**, 1353–1368.
- [15] F. Moro, D. P. Mills, S. T. Liddle, J. van Slageren, *Angew. Chem. Int. Ed.* **2013**, *52*, 3430–3433; *Angew. Chem.* **2013**, *125*, 3514–3517.
- [16] Web CS Web CSD v.1.1.1 (search date 20th June 2014): I. R. Thomas, I. J. Bruno, J. C. Cole, C. F. McRae, E. Pidcock, P. A. Wood, *J. Appl. Crystallogr.* **2010**, *43*, 362–366.
- [17] a) S. D. Gabelnick, G. T. Reedy, M. G. Chasanov, *J. Chem. Phys.* **1973**, *59*, 6397–6404; b) M. Zhou, L. Andrews, N. Ismail, C. Marsden, *J. Phys. Chem. A* **2000**, *104*, 5495–5502.
- [18] P. Pyykkö, J. Li, N. Runeberg, *J. Phys. Chem.* **1994**, *98*, 4809–4813.
- [19] a) E. F. Hayes, *J. Phys. Chem.* **1966**, *70*, 3740–3742; b) C. A. Coulson, *Isr. J. Chem.* **1973**, *11*, 683–690; c) C. E. Meyers, L. J. Norman, L. M. Loew, *Inorg. Chem.* **1978**, *17*, 1581–1584; d) R. L. De Kock, M. A. Peterson, L. K. Timmer, E. J. Baerends, P. Vernooijs, *Polyhedron* **1990**, *9*, 1919–1934.
- [20] R. J. Baker, *Coord. Chem. Rev.* **2012**, *256*, 2843–2871.
- [21] Full details can be found in the Supporting Information.
- [22] S. M. Mansell, B. F. Perandones, P. L. Arnold, *J. Organomet. Chem.* **2010**, *695*, 2814–2821.
- [23] C. J. Windorff, W. J. Evans, *Organometallics* **2014**, *33*, 3786–3791.
- [24] W. T. Carnall, *J. Chem. Phys.* **1992**, *96*, 8713–8726.
- [25] M. Karbowiak, J. Drożdżyński, *J. Alloys Compd.* **2000**, *300–301*, 329–333.
- [26] D. P. Mills, F. Moro, J. McMaster, J. van Slageren, W. Lewis, A. J. Blake, S. T. Liddle, *Nat. Chem.* **2011**, *3*, 454–460.
- [27] a) D. M. King, F. Tuna, E. J. L. McInnes, J. McMaster, W. Lewis, A. J. Blake, S. T. Liddle, *Science* **2012**, *337*, 717–720; b) H. Nakai, X. Hu, L. N. Zakharov, A. L. Rheingold, K. Meyer, *Inorg. Chem.* **2004**, *43*, 855–857.
- [28] Crystal data for 1: C₃₆H₉₀N₃Si₆U, *M*_r = 971.67 g mol⁻¹, space group C2/c, *a* = 21.7732(11), *b* = 13.2453(8), *c* = 17.9674(9) Å, β = 110.972(6)°, *V* = 4838.4(5) Å³, *Z* = 4, ρ_{calcd} = 1.334 g cm⁻³; MoKα radiation, λ = 0.71073 Å, μ = 3.529 mm⁻¹, *T* = 150 K. 11360 points (5457 unique, *R*_{int} = 0.0567, 2θ < 57.6°). Data were collected on an Agilent Technologies Supernova diffractometer and were corrected for absorption (transmission 0.926–1.000). The structure was solved by direct methods and refined by full-matrix least-squares on all *F*² values to give *wR*² = {Σ[w(*F*_o² - *F*_c²)²]/Σ[w(*F*_o²)²]}^{1/2} = 0.0678, conventional *R* = 0.0486 for *F* values of 5457 with *F*_o² > 2σ(*F*_o²), *S* = 0.986 for 224 parameters. Residual electron density were 1.240 maximum and -1.355 e Å⁻³ minimum. CCDC-1015959 (1) contains the supplementary crystallographic data for this paper. These data can be obtained free of charge from The Cambridge Crystallographic Data Centre via www.ccdc.cam.ac.uk/data_request/cif.
- [29] D. C. Bradley, M. B. Hursthouse, P. F. Rodesiler, *J. Chem. Soc. D: Chem. Commun.* **1969**, 14–15.
- [30] W. G. van der Sluys, C. J. Burns, A. P. Sattelberger, *Organometallics* **1989**, *8*, 855–857.
- [31] a) E. D. Brady, D. L. Clark, J. C. Gordon, P. J. Hay, D. W. Keogh, R. Poli, B. L. Scott, J. G. Watkin, *Inorg. Chem.* **2003**, *42*, 6682–6690; b) L. Maron, O. Eisenstein, *New J. Chem.* **2001**, *25*, 255–258.
- [32] J. C. Green, M. Payne, E. A. Seddon, R. A. Andersen, *J. Chem. Soc. Dalton Trans.* **1982**, 887–892.
- [33] J. V. Ortiz, P. J. Hay, R. L. Martin, *J. Am. Chem. Soc.* **1992**, *114*, 2736–2737.
- [34] P. J. Hay, R. L. Martin, *J. Alloys Compd.* **1994**, *213*, 196–198.
- [35] A. Gavezzotti, *Acta Cryst.* **1996**, *B52*, 201–208.
- [36] a) D. F. Evans, *J. Chem. Soc.* **1959**, 2003–2005; b) S. K. Sur, *J. Magn. Reson.* **1989**, *82*, 169–173; c) D. H. Grant, *J. Chem. Educ.* **1995**, *72*, 39–40.
- [37] E. R. Jones, M. E. Hendricks, J. A. Stone, D. G. Karraker, *J. Chem. Phys.* **1974**, *60*, 2088–2094.
- [38] a) J. D. Rinehart, J. R. Long, *J. Am. Chem. Soc.* **2009**, *131*, 12558–12559; b) J. D. Rinehart, K. R. Meihaus, J. R. Long, *J. Am. Chem. Soc.* **2010**, *132*, 7572–7573; c) K. R. Meihaus, J. D. Rinehart, J. R. Long, *Inorg. Chem.* **2011**, *50*, 8484–8489; d) J. D. Rinehart, J. R. Long, *Dalton Trans.* **2012**, *41*, 13572–13574.
- [39] J. J. Baldoví, S. Cardona-Serra, J. M. Clemente-Juan, E. Coronado, A. Gaita-Arino, *Chem. Sci.* **2013**, *4*, 938–946.
- [40] H. D. von Amberger, S. Jank, H. Reddmann, N. M. Edelstein, *Mol. Phys.* **1997**, *90*, 1013–1026.
- [41] E. Lucaccini, L. Sorace, M. Perfetti, J. P. Costes, R. Sessoli, *Chem. Commun.* **2014**, *50*, 1648–1651.
- [42] P. B. Hitchcock, M. F. Lappert, L. Maron, A. V. Protchenko, *Angew. Chem. Int. Ed.* **2008**, *47*, 1488–1491; *Angew. Chem.* **2008**, *120*, 1510–1513.

Received: August 14, 2014

Published online on September 21, 2014